Modeling Microbial Regulatory Feedback in Organic Matter Decomposition Identifies Copiotrophic Traits as Key Drivers of Positive Priming

Firnaaz Ahamed[1,†], James C. Stegen[2,3,*], Emily B. Graham[2,4], Timothy D. Scheibe[2], Hyun-Seob Song[1,5,*]

[1]Department of Biological Systems Engineering, University of Nebraska–Lincoln, Lincoln, NE, United States.

[2]Earth and Biological Sciences Directorate, Pacific Northwest National Laboratory, Richland, WA, United States.

[3]School of the Environment, Washington State University, Pullman, WA, United States.

[4]School of Biological Sciences, Washington State University, Pullman, WA, United States.

[5]Department of Food Science and Technology, Nebraska Food for Health Center, University of Nebraska–Lincoln, Lincoln, NE, United States.

*Correspondence: James.Stegen@pnnl.gov (JCS); hsong5@unl.edu (H-SS)

†Current address: School of Engineering, Faculty of Innovation and Technology, Taylor's University, 47500 Subang Jaya, Malaysia.

Abstract

Microbial priming, characterized by significant changes in organic matter (OM) decomposition rates due to minor external treatments with the addition of labile OM, exerts a significant impact on biogeochemical cycles in ecosystems. Priming can take many forms, including positive priming (increased OM decomposition rates), negative priming (decreased OM decomposition rates), and everything in between. Currently, we lack generalizable frameworks that can mechanistically explain these diverse patterns of priming, making it challenging to identify its governing factors. In this work, we theorized priming to result from a biogeochemical feedback loop regulated by microorganisms optimizing the balance between cost and benefit towards maximizing their growth rates, i.e., the cost of exoenzyme synthesis for decomposing complex OM and the benefits of energy acquisition from microbial growth on labile OM. Accordingly, we examined the impacts of microbial growth traits and interactions on priming employing a cybernetic approach, which specializes in predicting complex microbial growth patterns through a regulatory feedback loop. Using the cybernetic model, we simulated the occurrence of priming driven by microorganisms in the following four distinct settings: copiotrophic degraders independently, oligotrophic degraders independently, a consortium of copiotrophic degraders and oligotrophic non-degraders, and a consortium of oligotrophic degraders and copiotrophic non-degraders. Comprehensive Monte Carlo simulations using these four models revealed several critical aspects of priming, including: (1) positive priming is a dominant phenomenon in general, while negative priming can also occur sporadically under specific parameter settings, (2) positive priming is more frequently observed in microbial systems with copiotrophic degraders than with oligotrophic degraders, (3) the presence of copiotrophic non-degraders suppresses positive priming, while the presence of oligotrophic non-degraders promotes positive priming, and (4) the evolution of priming over time is also influenced by microbial growth traits and interactions. Most strikingly, all four models predicted a dramatic positive priming effect triggered by the addition of a small amount (i.e., less than 10%) of labile organic matter, with no notable changes observed beyond this point. Together with other findings summarized above, this might represent a key feature of microbial priming that might be commonly observed across microbial systems with diverse growth traits as supported by literature data. Overall, this work combining new theories and models significantly enhances our understanding of priming by providing model-generated and empirically-testable hypotheses on the mechanisms governing priming.

Keywords: priming, metabolic regulation, growth traits, microbial interactions, cybernetic modeling

1. Introduction

Natural ecosystems often show significant changes in the decomposition rate of organic matter (OM) when stimulated by the addition of easily degradable labile OM, a phenomenon termed priming. The resulting increased and decreased OM decomposition rates represent positive and negative priming, respectively (Bingeman et al., 1953; Kuzyakov et al., 2000). The occurrence of priming has been frequently reported in the literature. For example, labile OM in the form of plant litter and root exudates triggers priming, accelerating the microbial decomposition of complex soil OM, which benefits plant growth and soil quality by facilitating nutrient and energy exchange between microbial community and plants in the rhizosphere (Fontaine et al., 2003; Soong et al., 2020). Priming equally manifests in other ecological domains, such as sediments in hyporheic zones in rivers and deep ocean seabeds, which influence the nutrient and energy cycles (Graham et al., 2017). In the context of global warming, however, positive priming can have adverse implications, as it stimulates increased microbial respiration, leading to heightened carbon dioxide emissions from the decomposition of soil OM rich in carbon (Nottingham et al., 2009; King, 2011). Conversely, negative priming aids carbon sequestration efforts by preserving soil carbon from mineralization (Guenet et al., 2018; Liang et al., 2023).

Despite the great potential of exerting long-term effects on ecosystem dynamics and function (King, 2011), our understanding of fundamental mechanisms and key factors governing priming remains limited, posing challenges in accurately predicting biogeochemical dynamics. Priming can be driven by biotic and abiotic factors, including microbial traits (Nottingham et al., 2009; Fontaine et al., 2011), environmental constraints such as carbon limitations (Graham et al., 2017; Soong et al., 2020), nutrient limitations (Fontaine et al., 2011; Hicks et al., 2019; Feng et al., 2021), or combinations thereof. Although experimental evidence suggests that microbial traits and interactions can play pivotal roles in priming (Brant et al., 2006; Garcia-Pausas and Paterson, 2011; Yu et al., 2018; Hicks et al., 2019), the extensive diversity observed in natural ecosystems poses obstacles to completely resolving their effects on OM decomposition (Trivedi et al., 2013).

Priming occurs when the addition of external labile OM alters substrate uptake, affecting OM decomposition rates. Further, microbial regulation of exoenzyme synthesis for the decomposition of complex OM influences the production of labile OM, which in turn affects substrate utilization. Then, microbial growth traits, such as copiotrophs (fast-growing, thriving in nutrient-rich environments) and oligotrophs (slow-growing, adapted to nutrient-poor conditions), along with interactions, also significantly influence substrate utilization. Additionally, the presence of non-degraders in natural ecosystems that compete for substrates also impacts substrate dynamics (Momeni et al., 2013; Trivedi et al., 2013; Song et al., 2014). Therefore, to achieve a mechanistic understanding of priming, it is crucial to consider these fundamental microbial processes, such as growth traits, microbial interactions, regulated synthesis of exoenzymes, and the role of non-degraders, as key factors controlling priming (Fontaine et al., 2003; Brant et al., 2006; Garcia-Pausas and Paterson, 2011; Di Lonardo et al., 2017; Yu et al., 2018; Hicks et al., 2019). The limited consideration of microbial components in most studies hinders the elucidation

of priming mechanisms (Nottingham et al., 2009; Fontaine et al., 2011; Trivedi et al., 2013). Moreover, experimental approaches quantifying priming effects through changes in respiration rates as proxies for OM decomposition also face limitations due to the associated complexities with distinguishing real priming from apparent changes (i.e., microbial biomass turnover). In essence, there are currently no generalizable theories that fully explain the diverse patterns of priming effects, highlighting the need for mechanistic models capable of predicting both positive and negative priming within a unified framework.

In this regard, cybernetic modeling is of particular interest due to its unique capability of predicting complex microbial growth patterns in dynamically varying environments by accounting for metabolic regulation (Ramkrishna and Song, 2018). Instead of accounting for all molecular details of microbial regulation that are generally unknown, cybernetic models provide rational descriptions of regulation based on the cybernetic laws derived from an optimal control theory. The resulting cybernetic control laws dictate which enzymes microorganisms need to synthesize and activate in given environmental conditions to maximize their growth rates (Young and Ramkrishna, 2007). Rooted in an economic return-on-investment concept, cybernetic models predict microbial actions based on the balance between the cost of enzyme synthesis for decomposing complex OM and the benefit derived from acquiring energy for microbial growth on labile OM. Therefore, cybernetic modeling can serve as an ideal tool for exploring priming because it accounts for microbial regulation through a feedback loop comprising three key processes: enzyme synthesis, complex OM decomposition, and microbial growth on labile OM.

In this work, we proposed a novel theoretical framework that employs cybernetic modeling to predict microbial responses to the addition of labile OM and their impacts on the decomposition rates of chemically complex OM. Towards identifying key factors governing priming effects, we evaluate several questions: (1) how growth traits of microorganisms degrading complex OM drive positive and negative priming, (2) how the presence of non-degraders affect priming through interactions with degraders, (3) how the temporal patterns of priming are affected by these factors, and (4) whether any theoretical principles may be translatable across different microbial systems. To address these questions, we developed four models of microbial systems, comprising both single functional groups (copiotrophs or oligotrophs) and binary functional groups (copiotrophs and oligotrophs), all grounded in a unified framework, to explore how microbial growth traits and interactions influence priming rates. To draw unbiased conclusions, we conducted Monte Carlo simulations by assigning random parameter values to each model, rather than calibrating parameters with specific values that might be relevant to one system but not to others. The comprehensive simulations generated by this method provided new insights into each of the key questions, revealing several critical aspects of priming. In addition to examining the effects of microbial growth traits and interactions on priming, our models demonstrated the existence of a critical amount of labile OM (below around 10%) that dramatically triggers positive priming in the decomposition of complex OM, a consistent finding across all four models, regardless of the types of microbial growth traits and interactions.

2. Methods

2.1. Model equations

For generality, we provide the model equations only for a binary consortium composed of microbial species *i* and *j* representing mixed growth traits because the single functional group models are readily derivable from the consortium model by removing one of the species. The growth of species *i* in the consortium in a uniformly mixed batch environment is represented as:

$$\frac{dX_i}{dt} = r_{S,i} Y_{X,i} X_i \tag{1}$$

where the subscript *i* denotes the ith species, X_i, $Y_{X,i}$, and $r_{S,i}$ represent biomass concentration, biomass yield, and specific growth rate, respectively. The mass balance of the labile OM is given by:

$$\frac{dS}{dt} = Y_S \sum_i r_{Z,i} - \sum_i r_{S,i} X_i \tag{2}$$

where Y_S is the yield of labile OM from the degradation of complex OM, $r_{Z,i}$ is the rate of degradation of complex OM by species *i*, and $r_{S,i}$ is the specific uptake rate of labile OM in species *i*. Accordingly, the degradation of complex OM is given as:

$$\frac{dZ}{dt} = -\sum_i r_{Z,i} \tag{3}$$

The degradation of complex OM and the assimilation of labile OM is regulated by exoenzymes and endoenzymes, respectively:

$$\frac{dE_i}{dt} = \alpha_{E,i} X_i + u_{E,i} Y_{E,i} r_{S,i} X_i - \beta_{E,i} E_i \tag{4}$$

$$\frac{de_i}{dt} = \alpha_{e,i} + u_{e,i} Y_{e,i} r_{S,i} - \beta_{e,i} e_i \tag{5}$$

Here, $\alpha_{E,i}$ and $\alpha_{e,i}$ are the constitutive (basal) enzyme synthesis rates, $Y_{E,i}$ and $Y_{e,i}$ are the enzyme yields, and $\beta_{E,i}$ and $\beta_{e,i}$ are the enzyme decay rates. Then, the specific uptake rate of labile OM and the degradation rate of complex OM are given in the form of Michaelis-Menten kinetics:

$$r_{S,i} = k_{S,i} \frac{\left(S/K_{S,i}\right)}{1+\left(S/K_{S,i}\right)} \frac{\left(e_i/K_{e,i}\right)}{1+\left(e_i/K_{e,i}\right)} \tag{6}$$

$$r_{Z,i} = k_Z \frac{\left(Z/K_Z\right)}{1+\left(Z/K_Z\right)} \frac{\left(E_i/K_{E,i}\right)}{1+\left(E_i/K_{E,i}\right)} \tag{7}$$

Here, $k_{S,i}$ and k_Z are the maximum rates of labile OM update and complex OM decomposition, respectively, and $K_{S,i}$ and $K_{e_S,i}$ are their associated saturation constants.

In single functional group models, we consider that microorganisms can degrade complex OM (i.e., degraders). In binary consortium models, we consider one species to be a degrader and the other species to be a non-degrader. We also use the term cheaters to denote non-degraders because they exploit the benefits from degraders by competitively consuming the produced labile OMs without contributing to the degradation of complex OM (Momeni et al., 2013; Trivedi et al., 2013; Song et al., 2014).

2.2 Parameter assignment and simulation settings

Variability in model parameter values leads to drastically different results in the context of priming effects. Therefore, predicting priming outcomes is challenging even with known microbial growth traits and environmental conditions. To address this, we generate model results using Monte Carlo simulations by assigning random values to model parameters across different environmental conditions except the kinetic parameters associated with microbial growth. That is, to reduce the complexity of analysis, we fixed the labile OM uptake kinetic parameters ($k_{S,i}$, $K_{S,i}$) to distinguish the growth traits between oligotrophs and copiotrophs (see **Supplementary Text** and **Supplementary Figure S1**). Similarly, we fixed the exoenzyme synthesis kinetics to differentiate between degraders ($\frac{dE_i}{dt} \neq 0$) and non-degraders ($\frac{dE_i}{dt} = 0$) based on their ability to synthesize exoenzymes. Combination of the role of microorganisms (as degraders or cheaters) with copiotrophic and oligotrophic growth traits based on this pre-chosen parameter setting generates the four major players to be considered in simulations, including copiotrophic degrader (CD), copiotrophic cheaters (CC), oligotrophic degrader (OD), and oligotrophic cheater (OC). To ensure a fair comparison between different test cases, the initial microbial concentrations are made equal between the two microbial groups in the binary consortia. The same concentrations are also used in the single functional group models as well, meaning the total biomass concentration in these models is half that of the consortium models.

Importantly, the complex OM degradation kinetic parameters (k_Z, K_Z, Y_S) are also fixed to ensure that this study focuses solely on the variability in the growth traits of the microbes affecting the priming outcome, rather than the variability in complex OM properties. To represent the degradation of complex OM and the production of labile OM, Y_S must be greater than 1 (synonymous with the degradation of long-chain polymers into shorter oligomers or monomers), but using different values would only adjust the magnitude of priming without altering the qualitative trends. In other words, only the exoenzyme and endoenzyme synthesis kinetic parameters are randomized in the Monte Carlo simulations. By stochastically assigning values to

the remaining model parameters within prescribed ranges using a uniform distribution, we investigated the combined effects of microbial cost-benefit regulations and interactions between microbial groups with distinct growth traits on priming outcomes. To vary the environmental conditions to manifest different priming patterns, we varied the mixing fraction of labile OM with complex OM from 0 to 1, representing a mixture with pure complex OM and pure labile OM, respectively. In all cases, the Monte Carlo simulation results are based on no less than 200 runs for each mixture. The values of all model parameters, including those that were fixed or the bounds for randomized parameters, are collated in **Supplementary Table S1**.

2.3 Representation of microbial regulation using cybernetic modeling

The cost-benefit regulation of exoenzyme synthesis, and energy acquisition from microbial growth achieved from the assimilation of labile OM through the synthesis of exo- and endoenzymes in Eqs. (4) and (5), is governed by cybernetic variables $u_{E,i}$ and $u_{e,i}$, respectively, where $u_{E,i} + u_{e,i} = 1$. We employ generalized cybernetic laws based on optimal control systems, enabling the representation of microorganisms' evolutionary strategy to regulate their metabolism in the interest of future returns over a finite time horizon (Young and Ramkrishna, 2007). This modeling capability is particularly crucial in complex substrate environments, where the investment of invaluable cellular resources in synthesizing complex OM-degrading exoenzymes does not yield immediate returns in terms of cell growth but is necessary for future growth when degraded products (labile OM) become available for assimilation. The detailed formulation of optimal control-based generalized cybernetic regulation is given in Young and Ramkrishna (2007), but briefly:

$$\begin{aligned} \mathbf{A} &= \frac{\partial \mathbf{f}}{\partial \mathbf{x}}\left(\mathbf{x}(t), \mathbf{u}_i\right) \\ \mathbf{B}_{\mathbf{u}_i} &= \frac{\partial \mathbf{f}}{\partial \mathbf{u}_i}\left(\mathbf{x}(t), \mathbf{u}_i\right) \\ \mathbf{p}_{\mathbf{u}_i} &= \mathbf{B}_{\mathbf{u}_i}^{\mathrm{T}} \mathbf{e}^{\mathbf{A}^{\mathrm{T}}\Delta t} \mathbf{q} \end{aligned} \tag{8}$$

Here, f is the system of ordinary differential equations in Eqs. (1) – (5), x is the state vector of the system, $u_i = \left[u_{E,i}, u_{e,i}\right]^T$, and q is the vector representing the metabolic objective of the system, which in this work is the cell growth rate of the respective microbial groups (Eq. (1)). The future finite time horizon across which the returns are evaluated is computed based on the minimum time scale of the system, i.e.,

$$\Delta t = \frac{1}{\mu(\mathbf{A})} \tag{9}$$

where $\mu(A)$ is the maximum eigenvalue of A. Subsequently, the cybernetic variables are evaluated using matching law over the return-on-investment of finite cellular resources:

$$\mathbf{u}_i = \frac{\mathbf{p}_{\mathbf{u}_i}}{\left\| \mathbf{p}_{\mathbf{u}_i} \right\|_1} \tag{10}$$

2.4 Metrics for quantifying model-estimated priming effects

Priming effects refer to the change in the decomposition rate of complex OM when labile OM is added to the system. Experimental studies of priming effects often face limitations as they rely on changes in microbial respiration rates as a proxy for OM decomposition, which may not be ideal. However, in our modeling framework, we can directly quantify the overall relative priming effects by comparing the amounts of degraded complex OM in perturbed and unperturbed systems over a specified period:

$$P_{rel} = \frac{\Delta Z_a\left(t_\infty\right) - \Delta Z_c\left(t_\infty\right)}{\Delta Z_a\left(t_\infty\right) + \Delta Z_c\left(t_\infty\right)} \tag{11}$$

Here, ΔZ_a and ΔZ_c are the amended (treated with exogenous labile OM) and control amount of degraded complex OM evaluated at a time t_∞, respectively. Here, the overall relative priming effect is normalized such that the maximum positive priming ($P_{rel} = +1$) is achieved when $\Delta Z_a \gg \Delta Z_c$, maximum negative priming ($P_{rel} = -1$) is attained when no amended complex OM is degraded ($\Delta Z_a = 0$), and no priming effect ($P_{rel} = 0$) is observed when $\Delta Z_a = \Delta Z_c$. For special cases where $\Delta Z_a = \Delta Z_c = 0$, we assign no priming effect, i.e., $P_{rel} = 0$. To compare the priming effects consistently across test cases with different complex OM decomposition dynamics following the stochastic modeling, we define t_∞ as the moment when the complex OM is depleted to within a fixed tolerance:

$$\frac{\left(Z_a\left(t_\infty\right)/K_Z\right)^{n_Z}}{1+\left(Z_a\left(t_\infty\right)/K_Z\right)^{n_Z}} < 10^{-3} \tag{12}$$

The threshold above is low enough that it will no longer drive priming in the system unless external disturbances are re-introduced. Subsequently, the instantaneous relative priming effects are represented as:

$$P_{ins}\left(t_j\right) = \frac{\left[\Delta Z_a\left(t_j\right) - \Delta Z_a\left(t_{j-1}\right)\right] - \left[\Delta Z_c\left(t_j\right) - \Delta Z_c\left(t_{j-1}\right)\right]}{\Delta Z_c\left(t_\infty\right) + \Delta Z_c\left(t_\infty\right)}; \quad j = 2, 3, \ldots, \infty \tag{13}$$

where the overall relative priming effects and the instantaneous relative priming effects are associated such that $P_{rel} = \sum_{j=2}^{\infty} P_{ins}\left(t_j\right)$.

3. Results

3.1 Theoretical framework for systematic investigation of the impact of microbial growth traits and interactions on priming effects

The occurrence of positive or negative priming is dependent on both chemical and biological parameters. While a major chemical parameter in this setting is the mixing of relative amounts of complex and labile OM (**Fig. 1A**), the influence of microbial growth traits and interactions is also critical. It is of particular importance to account for metabolic regulation in microorganisms as we theorize that priming arises from microbial regulatory responses that balance the cost and benefit of decomposing complex OM and assimilating labile OM, respectively (**Fig. 1B**).

We formulated our modeling framework to include the following three fundamental microbial processes: synthesis of extracellular enzymes (or exoenzymes), the decomposition of complex OM, and the microbial growth on labile OM (**Fig. 1A**). These processes interact with each other through a closed feedback loop (Ahamed et al., 2021). Microorganisms synthesize exoenzymes to break down complex OM, producing labile OM that can be readily assimilated to support cell growth. In unprimed conditions, this feedback loop is inactive or slow, but when perturbed by the addition of exogenous labile OM, microorganisms gain additional energy to support growth and synthesize further exoenzymes, potentially facilitating positive priming by accelerating the decomposition of complex OM. However, the feedback loop will be suppressed if the return on degrading complex OM is not favorable to support cell growth, potentially leading to negative priming. The analysis of priming becomes complex when extending to microbial systems including multiple functional groups. Indeed, heterotrophic degraders in natural ecosystems often interact with other microbial groups such as non-degraders (or cheaters) (**Fig. 1B**).

Moreover, different microbial groups also have unique growth traits characterized by ecological attributes, such as copiotrophs and oligotrophs. Therefore, we further expound in this framework the possibility that the combined microbial cost-benefit regulations and interactions between microbial groups with distinct growth traits lead to various patterns of priming effects. While the number of cases we need to consider is large, as individual microbial functional groups have distinct growth traits characterized by copiotrophs and oligotrophs, we focus this study on the following cases, as they offer the greatest insights into the priming effects: single functional groups (**Fig. 1C**) consisting of (1) a degrader with copiotrophic growth traits (CD), and (2) a degrader with oligotrophic growth traits (OD); binary consortia (**Fig. 1D**) consisting of (3) a pair of CD and OC, and (4) a pair of CC and OD. We also assessed other binary consortia including OD-OC, CD-CC, and CD-OD to cover the full combinations (**Supplementary Fig. S2**).

3.2 Copiotrophic microbial growth traits promote strong positive priming

We examined how priming is affected by the growth traits of degraders, i.e., copiotrophs and oligotrophs, using the single functional group models illustrated in **Fig. 1C**. We compared the levels of overall relative priming (P_{rel}) and biomass concentrations (X) as a function of mixing fractions of labile OM (ν) with complex OM, between the CD and OD models in **Fig. 2**. Positive and negative values of P_{rel} represent the occurrence of positive and negative priming, respectively.

Both models (top panels of **Fig. 2**) predicted that the average P_{rel} values were zero at unmixed conditions as expected, i.e., $\nu = 0$ with pure complex OM or $\nu = 1$ with pure labile OM. The values drastically increased around $\nu \approx 0.1$, indicating that a small addition of exogenous labile OM (less than 10%) may be sufficient to trigger significant positive priming. The values then remained almost constant until reaching the maximum around $\nu \approx 0.97$. The presence of varying levels of priming, especially maximum positive priming, suggests that the addition of labile OM has a trade-off effect on priming. Specifically, certain levels of labile OM are required for triggering positive priming and reaching maximum positive priming, where the benefits outweigh the cost of expending microbial resources.

The CD model predicted the prevalence of positive priming, while also showing instances where P_{rel} values are zero, depending on the parameter sets randomly assigned in individual Monte Carlo simulations (top panel of **Fig. 2A**). The OD model also predicted the dominance of positive priming, but showed many instances where individual P_{rel} values are negative, resulting in lower average P_{rel} values compared to the CD model (top panel of **Fig. 2B**). Together, these results indicate that the positive priming can commonly occur with degraders exhibiting both copiotrophic and oligotrophic growth traits, though it is more facilitated by the former.

Meanwhile, CD and OD exhibited almost comparable growth over the entire range of the mixing fractions (bottom panels of **Fig. 2**). Owing to the inherent growth traits of copiotrophs and oligotrophs, the population level of CD is low at pure complex OM ($\nu = 0$), while the population level of OD is higher. However, at pure labile OM ($\nu = 1$), their population levels are comparable because, in the absence of complex OM to mine for additional labile OM, only the addition of exogenous labile OM remains for growth. Similar to the trend of the average P_{rel}, the population levels of OD and CD significantly increased around $\nu \approx 0.01$, plateaued between $\nu \approx 0.01$ and 0.97, and showed no appreciable growth as ν approaches 1. Despite these general similarities, the average P_{rel} values and population densities showed major differences in the delicate shapes of their profiles. In contrast with the average P_{rel} profiles showing a slight increase in the plateau, biomass concentration profiles showed a slight decline. This resulted in different optimal mixing fractions for maximizing the average P_{rel} and biomass concentrations. The former peaked around $\nu \approx 0.97$, while the latter reached its maximum around $\nu \approx 0.1$. This indicates that although one of the major factors driving microbial priming is the concentration of biomass (i.e., predominance of microorganisms), their delicate control is not always synchronized. As degraders must expend significant microbial resources to degrade complex OM to achieve maximum positive priming, this leaves relatively less energy available for growth, resulting in lower population levels.

3.3 The impact of microbial interactions on priming is dependent on growth traits

We extended our analysis to two mixed consortia composed of degraders and cheaters (as illustrated in **Fig. 1D**) to examine how their growth traits and interactions affect priming. We initially hypothesized that the presence of cheaters would suppress positive priming by weakening positive feedback loops, with the extent of suppression dependent on the growth traits of the two functional groups. Our models show that this hypothesis is only partially true. In fact, we observed the opposite in the CD-OC consortium, i.e., positive priming is promoted, as indicated by the higher average P_{rel} values (top panel of **Fig. 3A**), compared to the CD model (top panel of **Fig. 2A**). In contrast, we observed the frequent occurrence of negative priming in the OD-CC consortium, resulting in lower average P_{rel} values (top panel of **Fig. 3B**), compared to the OD model (top panel of **Fig. 2B**), in support of our hypothesis.

In the CD-OC consortium, the growth of cheaters was outcompeted by degraders (bottom panel of **Fig. 3A**). This was consistently observed over the entire range of ν, while the extent was more prominent at higher mixing fractions, conditions where CD can have growth advantages over OC. In contrast, the population densities of degraders and cheaters showed negative correlations in the OD-CC consortium along the mixing fraction (bottom panel of **Fig. 3B**). While OD grew more effectively than CC at low values of mixing fractions, the dominance of degraders did not lead to increased priming due to the intrinsic nature of OD, which is less effective at promoting positive priming. Moreover, the level of positive priming is nearly the same at higher values of ν, where CC grows more effectively than OD.

3.4 Temporal priming effects are shaped by microbial growth traits and interactions

In the prior two sections, we quantified overall relative priming over a specified reaction period, determined by an end time point, t_∞ (see **Methods**). However, priming effects are time-sensitive phenomena that depend on the period over which they are evaluated (Zhang et al., 2017), influencing both the magnitude and sign of P_{rel} values. The overall priming is merely the summation of instantaneous priming effects at each time point over a given period. Therefore, exploring the time dependency of priming is of critical importance in quantifying priming effects across systems with different timescales.

In this section, we examined the temporal changes of instantaneous relative priming (P_{ins}) among four priming models: CD only (**Fig. 4A**), OD only (**Fig. 4B**), CD-OC consortium (**Fig. 4C**), and OD-CC consortium (**Fig. 4D**), with three different mixing fractions ($\nu = 0.1$, 0.5, and 0.9). In all cases, the average P_{ins} exhibits a bell-shaped trend, i.e., gradually increasing to a certain point and then decreasing. When the microbial system is positively primed, complex OM is rapidly degraded (relative to the control) at the onset of the process, and the degradation slows down as the complex OM nears depletion, resulting in a bell-shaped priming observation. Furthermore, the

occurrences of negative average P_{ins} are more prevalent when the proportion of exogenous labile OM in the mix was high, especially during the later phases, when positive priming weakened.

Dynamic trends of priming are primarily dependent on the growth traits of degraders involved in the process. For example, the timing of maximum positive priming is consistent across mixing fractions in the CD and CD-OC models, where degraders exhibit copiotrophic growth traits (**Figs. 4A** and **4C**). In contrast, in the OD and OD-CC models, where degraders have oligotrophic growth traits, the peak times of positive priming shifted to later times with higher mixing fractions (**Figs. 4B** and **4D**) This is because CDs are more adept at labile OM-rich conditions when exogenous labile OM is added to the system, leading to quicker degradation of complex OM, compared to OD whose dynamics are slower under the same conditions.. Interestingly, positive priming was more prominent when CD was co-growing with OC (**Fig. 4C**), compared to the case with CD alone (**Fig. 4A**). However, those synergies between degraders and cheaters were not observed from the systems with OD (**Fig. 4B** vs. **4D**), similar to our observations of the overall relative priming effects in **Fig 3**.

4. Discussion

Despite extensive research in the past, key mechanisms and factors governing priming in general contexts remain elusive due to several challenges and complexities to overcome, including (1) the influence of numerous biotic and abiotic factors on priming, (2) difficulties in modeling the dynamics of microbial communities composed of various microbial functional groups with distinct growth traits, and (3) unknown process variables associated with microbial OM decomposition. A new theoretical and modeling framework developed in this work enables systematic investigation in a large parameter space to extract common and unique features of priming phenomena. With a focus on revealing the impacts of key chemical and biological parameters (such as mixing fractions of complex and labile OM, and microbial growth traits and interactions), we developed dynamic models of OM decomposition involving single functional microbial groups and consortia with distinct growth traits (copiotrophs and oligotrophs). We theorized the feedback loops of OM decomposition regulated by microorganisms to be a fundamental mechanism controlling the priming effects, which were incorporated into modeling using the cybernetic modeling framework. This new concept of microbial and OM decomposition model revealed several critical aspects of priming and offered new insights as detailed in the following sections.

4.1 Prevalence of positive priming and sporadic negative priming effects

Our modeling study shows that positive priming is prevalent in all test cases, and a small (less than 10%) addition of exogenous labile OM is sufficient to sustain significant positive priming effects (top panels of **Figs. 2 and 3**). This can be intuitively explained using the cybernetic perspective, as the microbial regulatory feedback loop shown in **Fig. 1B** is readily activated by degraders with either copiotrophic or oligotrophic growth traits by the addition of more

bioavailable labile OM. The degraders gain a quick and easy boost of energy from the assimilation of exogenous labile OM, allowing them to rapidly synthesize exoenzymes that degrade complex OM. This process produces more labile OM and perpetuates the feedback loop. This positive loop continues until the benefits of exoenzyme synthesis no longer outweigh the costs due to the significant depletion of complex OM. From an alternative perspective, it is apparent that the benefits of OM decomposition inherently always outweigh the costs of exoenzyme production, even when exogenous labile OM is not introduced, due to the potential future growth that can be achieved from labile products generated in the degradation process. However, there may not be enough available energy to synthesize the exoenzymes initially. The presence of exogenous labile OM removes this energy limitation, which is the fundamental working principle of positive priming.

On the other hand, negative priming is sporadic and therefore not observed in averaged results, but it is observed in individual runs of Monte Carlo simulations (top panels of **Figs. 2** and **3,** and **Fig. 4**). This occurs when microbes preferentially utilize labile OM to immediately support cell growth rather than synthesizing exoenzymes to degrade complex OM to produce more labile OM for future growth. As we operate on the basis that degraders regulate their metabolism with a focus on returns over a finite future time horizon achieved using cybernetic modeling based on optimal control systems (see **Methods**), microbes can anticipate future returns (Young and Ramkrishna, 2007), especially when complex substrates are involved. Therefore, from the cybernetic perspective, negative priming can only manifest when the cost of exoenzyme synthesis to degrade complex OM outweighs the future returns in terms of cell growth from the assimilation of labile OM from degraded complex OM. As previously mentioned, the addition of labile OM almost always removes the energy limitation for exoenzyme synthesis, making negative priming less common than positive priming. In negative priming, degraders lack the incentive to degrade complex OM and instead focus on consuming the available labile OM to build biomass.

4.2 Prevalence of negative priming in temporal dynamics

Instantaneous relative priming effects exhibit highly non-linear dynamics over time and are more likely to cross into the negative priming regime compared to the overall relative priming measure (**Fig. 4**). Particularly, temporal patterns of priming assume a bell-shaped curve, which can be explained as follows. By rapidly assimilating the labile OM, degraders gain an immediate energy boost to accelerate the degradation of complex OM, resulting in peak positive priming. This process leads to the accumulation of labile OM within the system. Microbes then allocate more energy towards consuming this labile OM in later phases, leading to a decrease in positive priming and the observed negative priming effect. Therefore, if the test cases in this study are evaluated over a different timeframe, it's plausible that we could observe altered priming outcomes, highlighting the importance of the time parameter in the priming phenomenon, and the dynamic nature of microbial interactions and their impact on OM decompositions. For instance, when examining the model results involving CD only and CD-OC consortia, which typically display

robust positive overall relative priming effects (top panels of **Figs. 2A and 3A**), instances of negative instantaneous relative priming effects can still be observed (**Figs. 4A and 4C**).

4.3 The impacts of microbial growth traits on positive and negative priming

Despite their distinct growth traits, CD and OD both utilize exogenous labile OM for a quick energy boost, enabling them to degrade complex OM into labile OM and sustain their populations. However, due to its preference for resource-rich niches, the positive regulatory feedback loop is strongly activated when CD are present, making CD more effective at achieving a positive priming effect (top panels of **Figs. 2A** and **3A**). Conversely, negative priming effects are observed when OD are involved in the process, whether independently or paired with CC, especially at higher labile OM loading (top panels of **Figs. 2B and 3B**). Oligotrophs are adapted to thriving in resource-poor conditions, so when confronted with high amounts of labile OM, they encounter more than they can consume. In this scenario, it is not beneficial for them to generate additional labile OM through the costly process of synthesizing exoenzymes. Instead, they focus on consuming the available labile OM for growth rather than secreting exoenzymes for complex OM degradation. However, when paired with CC, the extent and frequency of negative priming significantly increase (**Fig. 3B**). This occurs because CC rapidly consumes the exogenous and degraded labile OM, leaving insufficient energy for OD to continue degrading complex OM. On the contrary, the presence of OC enhanced the extent of positive priming by CD (top panel of **Fig. 3A**). This is also similarly observed in instantaneous relative priming effects (**Fig. 4C**).

With regards to microbial population densities, CD and OD exhibit almost comparable growth when considered independently (bottom panels of **Fig. 2**). Conversely, in mixed consortia, oligotrophs attain higher population levels than copiotrophs at low mixing fractions, and vice versa at high mixing fractions, as expected (bottom panel of **Fig. 3B**). The only exception is when CD is paired with OC, where the former dominates across all possible mixing fractions (**Fig. 3A**). This dominance occurs because the uptake of rich labile OM in OC is slower, preventing it from effectively capitalizing on the efforts of copiotrophic degraders in producing labile OM.

Additionally, when both CD and OD are paired together, the extent of positive priming is not as high, and occurrences of negative priming have significantly increased compared to the single functional group model of CD or the binary consortium of CD and OC (cf. top panels of **Supplementary Fig. S2A** with **Fig. 2A** and **Fig. 3A**, respectively). This can be explained by the presence of two degraders potentially leading to the accumulation of labile OM in the system, resulting in a decline in the degradation of complex OM. As expected from their characteristic growth traits, OD fare better in labile OM-poor conditions, while CD thrive in labile OM-rich conditions (bottom panel of **Supplementary Fig. S2A**).

However, when degraders and cheaters share similar growth traits, they compete equally for labile OM, resulting in less efficient triggering of positive priming effects, and increased chances of negative priming when compared with the single functional group models of the respective degraders (cf. top panels of **Supplementary Fig. S2** and **Fig. 2**). Similarly, the

combination of CD and CC tends to have a higher frequency of negative priming compared to when CD are paired with OC (cf. top panels of **Supplementary Fig. S2B** and **Fig. 3A**). This is because CC in the former are more adept at utilizing the labile OM produced by CD, thereby reducing the potential of positive priming. Also, CD and CC have comparable population levels as they both equally thrive and compete in labile OM-rich conditions (bottom panel of **Supplementary Fig. S2B**). However, the combination of OD and OC shows fewer instances of negative priming compared to when OD are paired with CC (cf. top panels of **Supplementary Fig. S2C** and **Fig. 3B**). This is because OC in the former are not accustomed to thriving on rich labile OM conditions, making them less effective in exploiting the degradation products produced by OD. This is also why OD fare better than OC in population levels (bottom panel of **Supplementary Fig. S2C)**.

Overall, priming outcomes can be complex given the combined effects of microbial regulation and interactions between microbial groups with distinct growth traits. However, to simplify, copiotrophs are generally associated with significant positive priming, while oligotrophs are linked to sporadic occurrences of negative priming. The summary of priming outcomes for all test cases in this study is provided in **Supplementary Table S2**.

4.4 A small addition of exogenous labile OM triggers significant positive priming

One of the common features of priming that we identified in our work, consistent across all test cases, is that significant positive priming is triggered by the addition of small amounts of labile OM (less than about 10%), beyond which no further significant improvements were observed. The presence of a small threshold to trigger significant positive priming explains why positive priming is more prevalent than negative priming. This is because the minimal amount of labile OM required to elicit a notable response makes it easier to achieve positive priming, while the conditions for negative priming often require more complex and less common scenarios. Moreover, this also reinforces the idea that the priming phenomenon results from a microbial regulatory response aimed at maximizing growth, where microbes strategically balance the cost and benefits trade-off to gain advantages from available resources.

When the addition of exogenous labile OM exceeds a certain threshold, there is more labile OM than degraders can consume. As a result, the system reaches a saturation point where degraders cannot further increase the exoenzyme synthesis rate, leading to no additional improvement in positive priming, even with more labile OM. Although this threshold may vary slightly between copiotrophs and oligotrophs, it is generally less than around 10% labile OM, depending on the fixed model parameters in this study. In addition, beyond the threshold where there is a surplus of labile OM, the motivation to further increase OM decomposition diminishes. As a result, microbes maintain their existing course of action, using the available labile OM to sustain exoenzyme synthesis and maintain the level of labile OM in the system through the degradation process.

Similar findings were evidently reported by Stegen et al. (2018), where the addition of up to only 10% labile OM-rich groundwater to complex OM-rich river water resulted in a significant increase in overall OM oxidation in the mixture. However, no further improvements in oxidation rate were observed beyond this 10% groundwater threshold. The increase in OM oxidation was also not significant below 10% groundwater, as it was inferred that the energy acquired from the assimilation of labile OM was insufficient to offset the energetic costs required to oxidize complex OM (Arrieta et al., 2015). Similarly, Guenet et al. (2010) suggested that the priming effect does not vary linearly with the addition of labile OM, instead, the amount of labile OM only partially controls priming, which functions as a saturating response. This closely resembles the observation in our study, where significant positive priming plateaus beyond a certain threshold. Likewise, Zhou et al. (2021) observed that frequently adding smaller amounts of labile OM resulted in a greater priming response than adding larger amounts less frequently. Lastly, one of the established mechanisms of positive priming is the acceleration of internal microbial metabolism by *trace amounts* of substrates, which leads to an immediate increase in microbial respiratory activity (Blagodatsky et al., 2010; Bernard et al., 2022), which further supports our findings in this study.

4.5 Conclusions

Overall, our study provides a novel theoretical framework that can be used to understand microbial priming effects in natural ecosystems. The identification of a critical threshold - where a minimal addition of labile organic matter can trigger significant positive priming - highlights the sensitivity of microbial communities to environmental changes and the potential for small perturbations to have significant impacts on biogeochemical cycles. These insights have broad implications for ecological modeling, carbon cycle research, and environmental management, particularly in the context of global climate change, where understanding the dynamics of carbon sequestration and release is paramount.

Nevertheless, we have developed our theoretical framework to systematically and specifically study the effects of microbial growth traits and interactions, contextualized within microbial regulatory mechanisms in the decomposition of complex OM. Consequently, some of our findings may be limited to the model conditions used in this study (fixed parameter values and constraints for randomized parameters representing copiotroph and oligotroph growth traits, complex OM properties, and complex OM degradation kinetics). There is potential for other significant observations to emerge when the model conditions are expanded to encompass a broader range of settings. For example, we have not considered the effects of steric hindrances of OM protected within the soil or mineral aggregates (Marschner and Kalbitz, 2003; Schmidt et al., 2011; Lavallee et al., 2020), or the mass transport of OM under non-uniform conditions. More importantly, it is important to consider the impact of OM stoichiometry and thermodynamic favorability on microbial processes and their implications on priming effects. Existing literature highlights how variations in OM composition, especially C/N ratios, can profoundly influence microbial activity (Ahamed et al., 2023) and the dynamics of priming (Fontaine et al., 2011; Abramoff et al., 2017; Hicks et al., 2019).

Future research should focus on integrating theoretical models with empirical data to test the hypotheses generated from this work to further refine our understanding of priming mechanisms and to develop more accurate predictions of ecosystem responses to environmental perturbations. We expect that the key concepts proposed in our framework will contribute significantly to the advancement of predictive ecological models aimed at understanding carbon and nutrient cycling in natural ecosystems.

AUTHOR CONTRIBUTIONS

All authors contributed to the design of the research. FA and H-SS developed the computational framework for exploring priming effects and drafted the article. FA developed numerical codes and performed computational simulations. The manuscript was reviewed, edited, and approved by all authors.

FUNDING

JCS, EBG, and TDS were supported by the U.S. Department of Energy, Office of Science, Office of Biological and Environmental Research, Environmental System Science (ESS) Program. This contribution originates from the River Corridor Scientific Focus Area (SFA) project at Pacific Northwest National Laboratory (PNNL). PNNL is operated by Battelle Memorial Institute for the U.S. Department of Energy under Contract DE-AC05-76RL01830. FA and H-SS were supported by the same through a subcontract with PNNL's River Corridor SFA.

CONFLICT OF INTEREST

The authors declare that the research was conducted in the absence of any commercial or financial relationships that could be construed as a potential conflict of interest.

REFERENCES

Abramoff, R.Z., Davidson, E.A., Finzi, A.C., 2017. A parsimonious modular approach to building a mechanistic belowground carbon and nitrogen model. Journal of Geophysical Research: Biogeosciences 122, 2418–2434. doi:10.1002/2017JG003796

Ahamed, F., Song, H., Ho, Y.K., 2021. Modeling coordinated enzymatic control of saccharification and fermentation by *Clostridium thermocellum* during consolidated bioprocessing of cellulose. Biotechnology and Bioengineering 118, 1898–1912. doi:10.1002/bit.27705

Ahamed, F., You, Y., Burgin, A., Stegen, J.C., Scheibe, T.D., Song, H.-S., 2023. Exploring the Determinants of Organic Matter Bioavailability through Integrative Modeling. Manuscript

under Review.
Arrieta, J.M., Mayol, E., Hansman, R.L., Herndl, G.J., Dittmar, T., Duarte, C.M., 2015. Dilution limits dissolved organic carbon utilization in the deep ocean. Science 348, 331–333. doi:10.1126/science.1258955
Bernard, L., Basile-Doelsch, I., Derrien, D., Fanin, N., Fontaine, S., Guenet, B., Karimi, B., Marsden, C., Maron, P.A., 2022. Advancing the mechanistic understanding of the priming effect on soil organic matter mineralisation. Functional Ecology 36, 1355–1377. doi:10.1111/1365-2435.14038
Bingeman, C.W., Varner, J.E., Martin, W.P., 1953. The Effect of the Addition of Organic Materials on the Decomposition of an Organic Soil. Soil Science Society of America Journal 17, 34–38. doi:10.2136/sssaj1953.03615995001700010008x
Blagodatsky, S., Blagodatskaya, E., Yuyukina, T., Kuzyakov, Y., 2010. Model of apparent and real priming effects: Linking microbial activity with soil organic matter decomposition. Soil Biology and Biochemistry 42, 1275–1283. doi:10.1016/j.soilbio.2010.04.005
Brant, J.B., Sulzman, E.W., Myrold, D.D., 2006. Microbial community utilization of added carbon substrates in response to long-term carbon input manipulation. Soil Biology and Biochemistry 38, 2219–2232. doi:10.1016/j.soilbio.2006.01.022
Di Lonardo, D.P., De Boer, W., Klein Gunnewiek, P.J.A., Hannula, S.E., Van der Wal, A., 2017. Priming of soil organic matter: Chemical structure of added compounds is more important than the energy content. Soil Biology and Biochemistry 108, 41–54. doi:10.1016/j.soilbio.2017.01.017
Feng, J., Tang, M., Zhu, B., 2021. Soil priming effect and its responses to nutrient addition along a tropical forest elevation gradient. Global Change Biology 1–14. doi:10.1111/gcb.15587
Fontaine, S., Henault, C., Aamor, A., Bdioui, N., Bloor, J.M.G., Maire, V., Mary, B., Revaillot, S., Maron, P.A., 2011. Fungi mediate long term sequestration of carbon and nitrogen in soil through their priming effect. Soil Biology and Biochemistry 43, 86–96. doi:10.1016/j.soilbio.2010.09.017
Fontaine, S., Mariotti, A., Abbadie, L., 2003. The priming effect of organic matter: A question of microbial competition? Soil Biology and Biochemistry 35, 837–843. doi:10.1016/S0038-0717(03)00123-8
Garcia-Pausas, J., Paterson, E., 2011. Microbial community abundance and structure are determinants of soil organic matter mineralisation in the presence of labile carbon. Soil Biology and Biochemistry 43, 1705–1713. doi:10.1016/j.soilbio.2011.04.016
Graham, E.B., Tfaily, M.M., Crump, A.R., Goldman, A.E., Bramer, L.M., Arntzen, E., Romero, E., Resch, C.T., Kennedy, D.W., Stegen, J.C., 2017. Carbon Inputs From Riparian Vegetation Limit Oxidation of Physically Bound Organic Carbon Via Biochemical and Thermodynamic Processes. Journal of Geophysical Research: Biogeosciences 122, 3188–3205. doi:10.1002/2017JG003967
Guenet, B., Camino-Serrano, M., Ciais, P., Tifafi, M., Maignan, F., Soong, J.L., Janssens, I.A., 2018. Impact of priming on global soil carbon stocks. Global Change Biology 24, 1873–1883. doi:10.1111/gcb.14069
Guenet, B., Neill, C., Bardoux, G., Abbadie, L., 2010. Is there a linear relationship between priming effect intensity and the amount of organic matter input? Applied Soil Ecology 46, 436–442.
Hicks, L.C., Meir, P., Nottingham, A.T., Reay, D.S., Stott, A.W., Salinas, N., Whitaker, J., 2019. Carbon and nitrogen inputs differentially affect priming of soil organic matter in tropical

lowland and montane soils. Soil Biology and Biochemistry 129, 212–222. doi:10.1016/j.soilbio.2018.10.015
King, G.M., 2011. Enhancing soil carbon storage for carbon remediation: Potential contributions and constraints by microbes. Trends in Microbiology 19, 75–84. doi:10.1016/j.tim.2010.11.006
Kuzyakov, Y., Friedel, J.K., Stahr, K., 2000. Review of mechanisms and quantification of priming effects. Soil Biology and Biochemistry 32, 1485–1498. doi:10.1016/S0038-0717(00)00084-5
Lavallee, J.M., Soong, J.L., Cotrufo, M.F., 2020. Conceptualizing soil organic matter into particulate and mineral-associated forms to address global change in the 21st century. Global Change Biology 26, 261–273. doi:10.1111/gcb.14859
Liang, Z., Rasmussen, J., Poeplau, C., Elsgaard, L., 2023. Priming effects decrease with the quantity of cover crop residues – Potential implications for soil carbon sequestration. Soil Biology and Biochemistry 184, 109110. doi:10.1016/j.soilbio.2023.109110
Marschner, B., Kalbitz, K., 2003. Controls of bioavailability and biodegradability of dissolved organic matter in soils. Geoderma 113, 211–235. doi:10.1016/S0016-7061(02)00362-2
Momeni, B., Brileya, K.A., Fields, M.W., Shou, W., 2013. Strong inter-population cooperation leads to partner intermixing in microbial communities. eLife 2, e00230. doi:10.7554/eLife.00230
Nottingham, A.T., Griffiths, H., Chamberlain, P.M., Stott, A.W., Tanner, E.V.J., 2009. Soil priming by sugar and leaf-litter substrates: A link to microbial groups. Applied Soil Ecology 42, 183–190. doi:10.1016/j.apsoil.2009.03.003
Ramkrishna, D., Song, H.-S., 2018. Cybernetic Modeling for Bioreaction Engineering, Cambridge Series in Chemical Engineering. Cambridge University Press, Cambridge.
Schmidt, M.W.I., Torn, M.S., Abiven, S., Dittmar, T., Guggenberger, G., Janssens, I.A., Kleber, M., Kögel-Knabner, I., Lehmann, J., Manning, D.A.C., Nannipieri, P., Rasse, D.P., Weiner, S., Trumbore, S.E., 2011. Persistence of soil organic matter as an ecosystem property. Nature 478, 49–56. doi:10.1038/nature10386
Song, H.-S., Cannon, W.R., Beliaev, A.S., Konopka, A., 2014. Mathematical Modeling of Microbial Community Dynamics: A Methodological Review. Processes 2, 711–752. doi:10.3390/pr2040711
Soong, J.L., Fuchslueger, L., Marañon-Jimenez, S., Torn, M.S., Janssens, I.A., Penuelas, J., Richter, A., 2020. Microbial carbon limitation: The need for integrating microorganisms into our understanding of ecosystem carbon cycling. Global Change Biology 26, 1953–1961. doi:10.1111/gcb.14962
Stegen, J.C., Johnson, T., Fredrickson, J.K., Wilkins, M.J., Konopka, A.E., Nelson, W.C., Arntzen, E.V., Chrisler, W.B., Chu, R.K., Fansler, S.J., Graham, E.B., Kennedy, D.W., Resch, C.T., Tfaily, M., Zachara, J., 2018. Influences of organic carbon speciation on hyporheic corridor biogeochemistry and microbial ecology. Nature Communications 9, 1–11. doi:10.1038/s41467-018-02922-9
Trivedi, P., Anderson, I.C., Singh, B.K., 2013. Microbial modulators of soil carbon storage: Integrating genomic and metabolic knowledge for global prediction. Trends in Microbiology 21, 641–651. doi:10.1016/j.tim.2013.09.005
Young, J.D., Ramkrishna, D., 2007. On the matching and proportional laws of cybernetic models. Biotechnology Progress 23, 83–99. doi:10.1021/bp060176q
Yu, Z., Chen, L., Pan, S., Li, Y., Kuzyakov, Y., Xu, J., Brookes, P.C., Luo, Y., 2018. Feedstock

determines biochar-induced soil priming effects by stimulating the activity of specific microorganisms. European Journal of Soil Science 69, 521–534. doi:10.1111/ejss.12542

Zhang, X., Han, X., Yu, W., Wang, P., Cheng, W., 2017. Priming effects on labile and stable soil organic carbon decomposition: Pulse dynamics over two years. PLoS ONE 12, 1–19. doi:10.1371/journal.pone.0184978

Zhou, J., Wen, Y., Shi, L., Marshall, M.R., Kuzyakov, Y., Blagodatskaya, E., Zang, H., 2021. Strong priming of soil organic matter induced by frequent input of labile carbon. Soil Biology and Biochemistry 152, 108069. doi:10.1016/j.soilbio.2020.108069

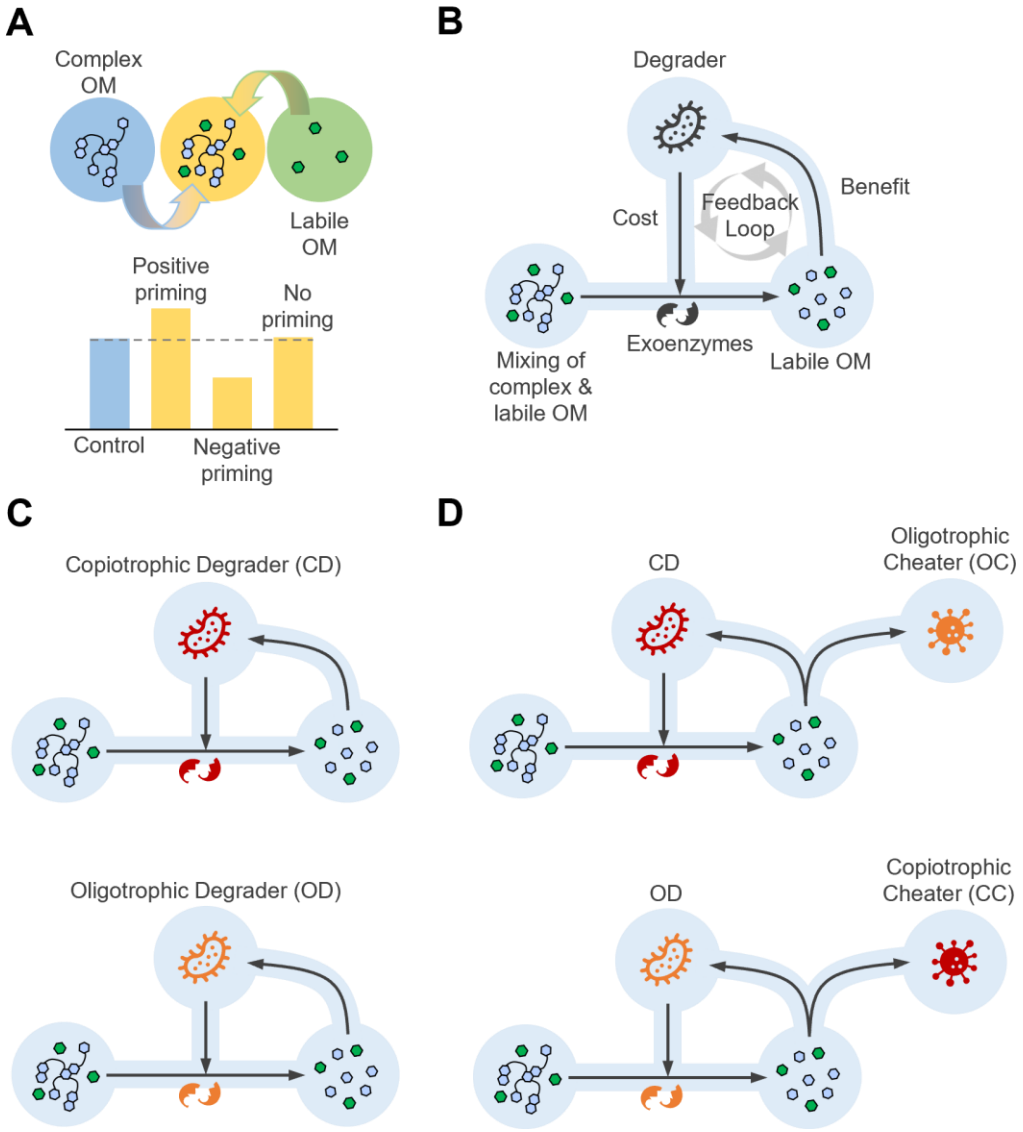

Figure 1. An illustration of a conceptual model developed to simulate priming effects driven by **(A)** chemical factors, specifically the mixing of complex and labile OM, which results in varied levels of complex OM decomposition rates, leading to positive, negative, or no priming. This process is governed by **(B)** microbial factors, i.e., dynamic cellular regulation through a closed feedback loop, which manages resources to balance the costs of exoenzyme synthesis for degrading complex OM and the benefits of assimilating produced labile OM for cell growth. Considering the influence of distinct microbial growth traits (oligotrophs and copiotrophs) and their interactions on priming, four major priming models are obtained depending on how copiotrophic and oligotrophic growth traits are assigned in **(C)** single functional groups with degraders alone, and **(D)** binary consortia with degraders and non-degraders (or cheaters).

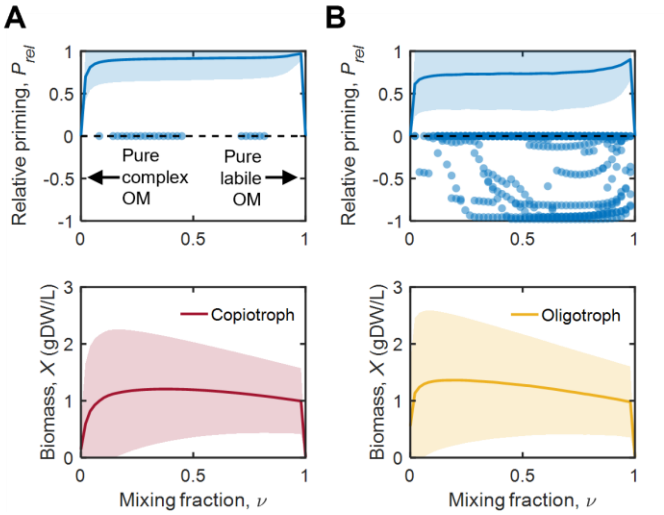

Figure 2. Overall relative priming effects and microbial population levels at various mixing compositions of complex and exogenous labile OM, evaluated for single functional group models of **(A)** copiotrophic degraders, and **(B)** oligotrophic degraders. The lines and shaded regions are averaged results and standard deviations of Monte Carlo simulations, respectively, while the markers are individual runs with negative overall relative priming effects.

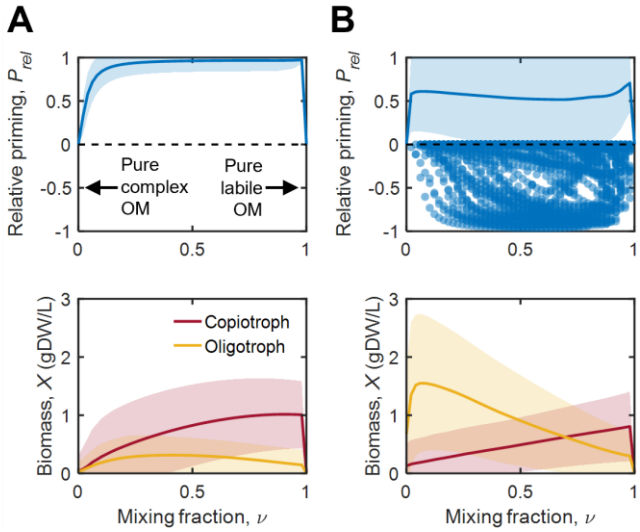

Figure 3. Overall relative priming effects and microbial population levels at various mixing compositions of complex and exogenous labile OM, evaluated for mixed cultures of **(A)** copiotrophic degrader and oligotrophic cheater, and **(B)** oligotrophic degrader and copiotrophic cheater. The lines and shaded regions are averaged results and standard deviations of Monte Carlo simulations, respectively, while the markers are individual runs with an overall negative priming effect.

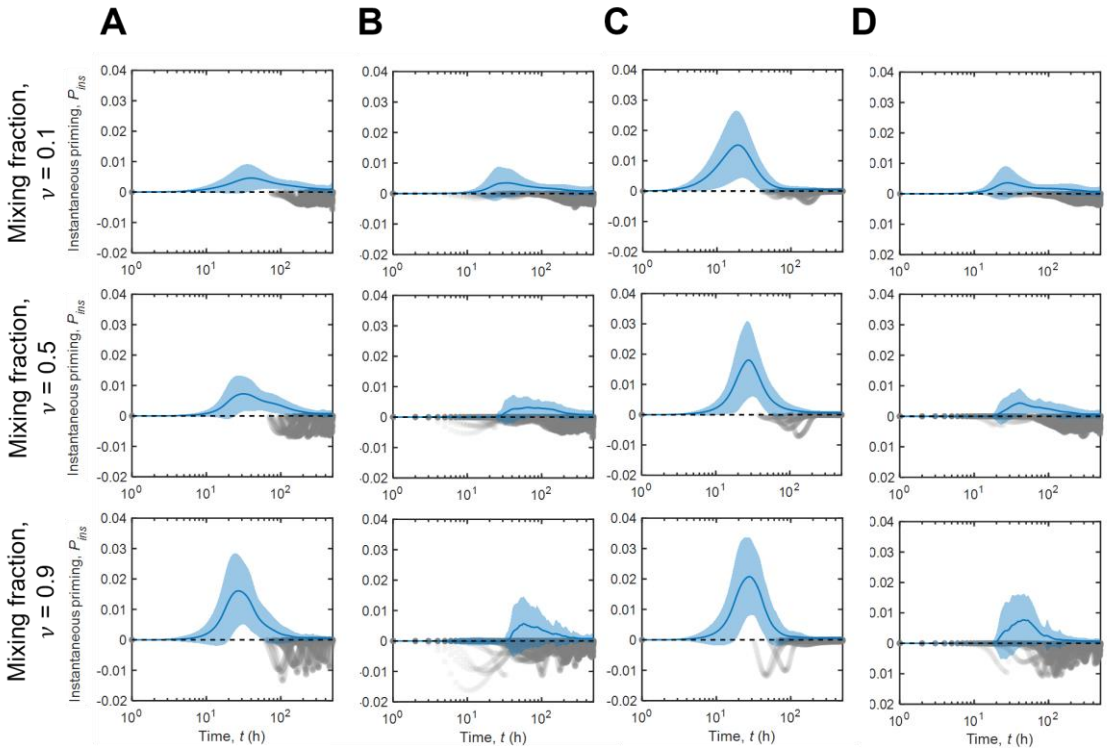

Figure 4. Instantaneous relative priming effects at low ($\nu = 0.1$), medium ($\nu = 0.5$), and high ($\nu = 0.9$) mixing compositions of exogenous labile OM with complex OM, evaluated for single functional group models of **(A)** copiotrophic degraders, **(B)** oligotrophic degraders, as well as binary consortia of **(C)** copiotrophic degrader and oligotrophic cheater, and **(D)** oligotrophic degrader and copiotrophic cheater. The lines and blue-shaded regions are averaged results and standard deviations of Monte Carlo simulations, respectively, while the gray-shaded markers indicate data points over time with negative instantaneous relative priming effects in individual runs.

SUPPLEMENTARY TEXT

Growth Traits of Copiotrophs and Oligotrophs

In **Supplementary Fig. S1**, we showed the behavior of oligotrophs and copiotrophs at varying labile organic matter (OM) concentrations and respective population levels based on our fixed parameter values. While oligotrophs and copiotrophs can thrive in environments with less than and more than 0.1 M of labile OM (**Supplementary Fig. S1A**), respectively, the microbes are also influenced by their respective population levels. The copiotrophs are more sensitive to changes in population levels, where they need to exceed the oligotroph population by more than three times under labile OM-limited conditions, and by 1.5 times under labile OM-rich conditions to equally compete for available labile OM **(Supplementary Fig. S1B**). Therefore, we set equal initial population levels for all microbial groups in all test cases in this study to give them equal footing in accessing labile OM (see **Methods**). However, the complex dynamics of complex OM degradation, simultaneous labile OM uptake, and microbial population accumulation can all influence the regulation strategy of microbes. Additionally, the degraders can transform the availability of labile OM for cheaters depending on their efficiency in degrading complex OM. Therefore, it is imperative that we not only use the end conditions to characterize the overall priming effects but also consider the transient changes in priming effects over time. The overall and transient priming outcomes for various test cases are explored in the **Results** section.

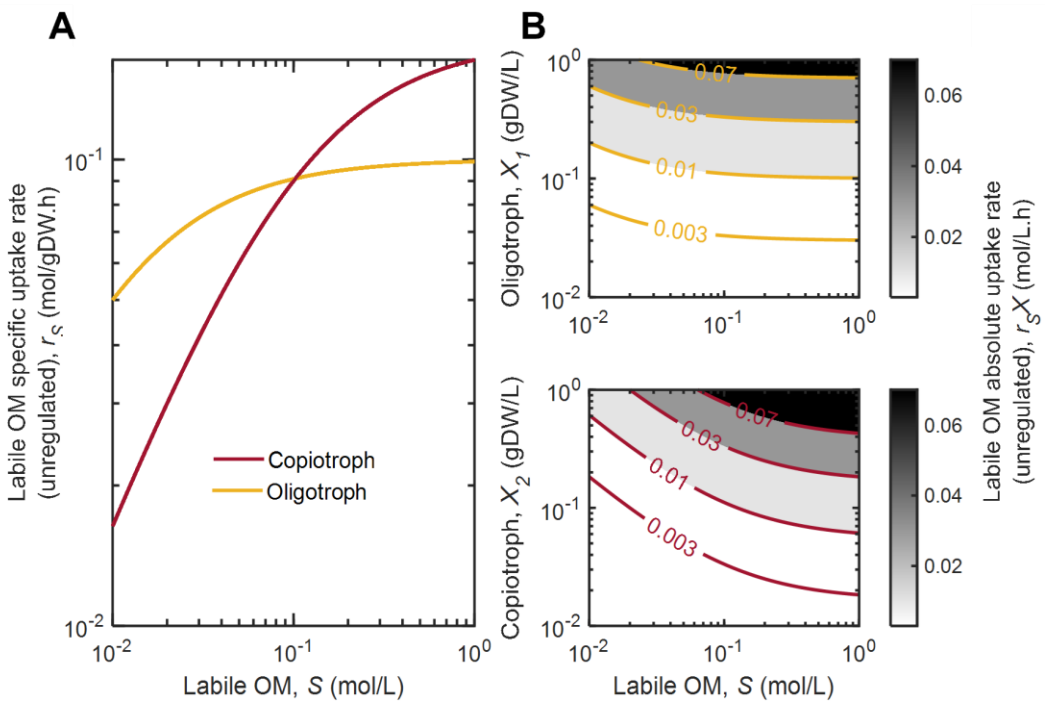

Supplementary Figure S1. Differences in labile OM uptake kinetics between oligotrophs and copiotrophs visualized as **(A)** unregulated specific uptake rates with respect to only labile OM levels, and **(B)** unregulated absolute uptake rates with respect to both biomass and labile OM levels.

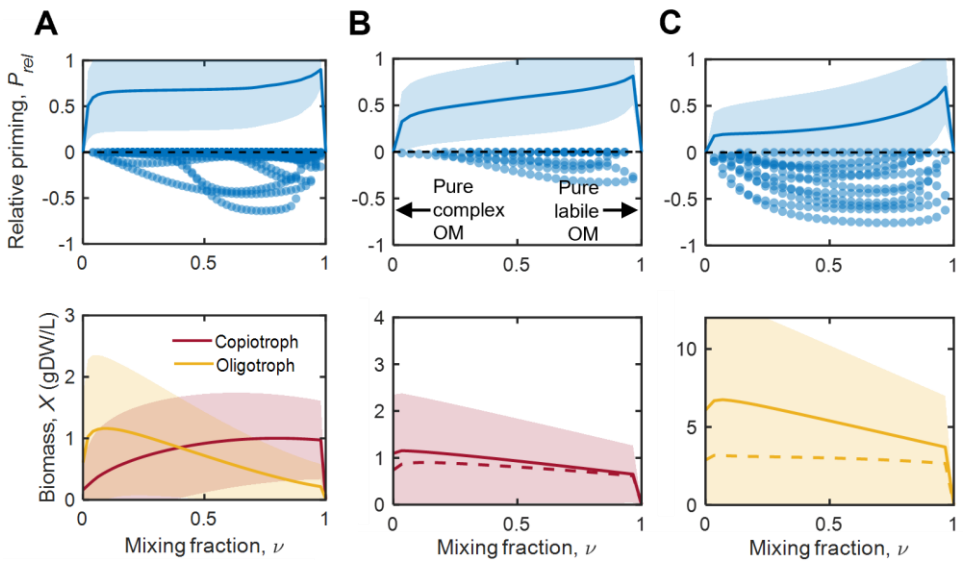

Supplementary Figure S2. Overall relative priming effects and microbial population levels at various mixing compositions of complex and exogenous labile OM, evaluated for binary consortia of **(A)** oligotrophic and copiotrophic degraders, **(B)** copiotrophic degraders and cheaters, and **(C)** oligotrophic degraders and cheaters. The lines and shaded regions are averaged results and standard deviations of Monte Carlo simulations, respectively, while the markers are individual runs with negative overall relative priming effects. In the population-level plots, the solid lines are degraders and dashed lines represent cheaters.

Supplementary Table S1. Model parameter values that were either fixed or randomized within specified bounds using uniform distributions in this study.

Model parameter	Fixed [F] or Randomized [R]	Copiotrophs	Oligotrophs	Remarks
$Y_{X,i}$	R	[0, 2]	[0, 2]	-
$k_{S,i}$	F	0.18	0.1	Copiotrophs > oligotrophs
$K_{S,i}$	F	0.1	0.01	Copiotrophs > oligotrophs
$\alpha_{E,i}$	R	[0, 1E-4]	[0, 1E-4]	-
$\alpha_{e,i}$	R	$= \alpha_{E,i}$	$= \alpha_{E,i}$	Assuming basal synthesis rates of exoenzymes and endoenzymes are identical for simplicity.
$Y_{E,i}$	R	[0, 2]	[0, 2]	-
$Y_{e,i}$	R	[0, 2]	[0, 2]	-
$\beta_{E,i}$	R	0.01	0.01	-
$\beta_{e,i}$	R	0.01	0.01	-
$K_{E,i}$	R	[0, 0.1]	[0, 0.1]	-
$K_{e,i}$	R	[0, 0.1]	[0, 0.1]	-
$X_i(0)$	F	0.01	0.01	Made equal for all microbial groups for a fair comparison.
$Z(0)$	F	Depending on the mixing fraction, ν		$\begin{cases} \nu = 0: Z(0) = 1, S(0) = 0 \\ \nu = 1: Z(0) = 0, S(0) = 1 \end{cases}$
$S(0)$	F			
k_Z	F	0.01		Fixed to exclude the effects of variability in complex OM properties on priming.
K_Z	F	0.1		
Y_S	F	2		

Supplementary Table S2. Summary of results for various priming models with different assortments of microbial groups exhibiting distinct growth traits. The levels of priming (low: $|P_{Rel}| < 0.1$, moderate: $|P_{Rel}| = 0.1 - 0.9$, high: $|P_{Rel}| > 0.9$) and the percentage occurrences of different priming types (positive, negative, zero) in the Monte Carlo simulations are presented. Note: CD – copiotrophic degrader; OD – oligotrophic degrader; CC – copiotrophic cheater; OC – oligotrophic cheater; PP – positive priming; NP – negative priming; ZP – zero priming.

	CD	OD
CD	PP: High levels, 96.0% NP: 0.0% ZP: 4.0%	PP: Moderate to high levels, 94.6% NP: Low to moderate levels, 1.4% ZP: 4.0%
OD	PP: Moderate to high levels, 94.6% NP: Low to moderate levels, 1.4% ZP: 4.0%	PP: Moderate to high levels, 95.7% NP: Low to high levels, 0.3% ZP: 4.0%
CC	PP: Low to moderate levels, 88.0% NP: Low to moderate levels, 5.3% ZP: 6.7%	PP: Moderate levels, 90.4% NP: Low to high levels, 5.6% ZP: 4.0%
OC	PP: High levels, 100.0% PP NP: 0.0% ZP: 0.0%	PP: Low to moderate levels, 82.9% NP: Low to moderate levels, 10.4% ZP: 6.7%